Synthesis of Amorphous and Nanostructured Cationic Polyacetylene/Silica Hybrids by Using Ionic Interactions

Tomoki Ogoshi and Yoshiki Chujo*

Department of Polymer Chemistry, Graduate School of Engineering, Kyoto University, Katsura, Nishikyo-ku, Kyoto 615-8510, Japan

Received February 9, 2005; Revised Manuscript Received August 22, 2005

ABSTRACT: Amorphous state optically transparent organic−inorganic polymer hybrids with a conducting, π-conjugated polymer of poly(2-ethynylpyridinium chloride) (P2EPY-HCl) were synthesized. The strong ionic interaction between the cationic pyridinium moieties of P2EPY-HCl and anionic silanol groups resulting from hydrolysis of tetramethoxysilane (TMOS) enabled the nanometer scale dispersion of P2EPY-HCl in a silica gel matrix. The homogeneity of the obtained P2EPY-HCl/silica hybrids was examined by SEM, tapping mode atomic force microscope (TM-AFM), and nitrogen adsorption porosimetry studies. The optical and thermal properties of the amorphous P2EPY-HCl/silica hybrids were investigated by UV and TGA measurements. Furthermore, nanostructured conducting-micelle/silica hybrids were obtained by using self-assembly of cationic polyacetylene having long alkyl chains (P2EPY-C18). Polyacetylene micelles (about 10 nm) were homogeneously dispersed in the siliceous phase.

Introduction

The chemistry of organic−inorganic nanocomposite and hybrid matters is nowadays a hot topic and attracts growing interest in basic material science due to their unique ability to combine chemistries between organic and inorganic fields and due to interfacial and confinement effects between the constituent phases.[1−4] One organic−inorganic hybrid subset includes organic−inorganic hybrid materials based on sol−gel processing using metal alkoxides.[4−15] The mild sol−gel process enables the preparation of organic−inorganic polymer hybrids with various polymers. A key point for the elaboration of organic−inorganic nanocomposite materials based on sol−gel processing is improving the affinity of the interface between the two phases. The low compatibility between organic species and inorganic materials often causes aggregation of the organic component in the inorganic host matrix during formation of the inorganic oxide from sol−gel processing.

Organic−inorganic hybrid materials based on sol−gel processing are studied in two main directions. One aim is to prepare hybrid materials by elaboration of amorphous materials at the molecular scale.[16−24] In our group, novel amorphous organic−inorganic polymer hybrids, where organic polymer is dispersed in an inorganic oxide, have been constructed using physical interactions such as hydrogen-bonding,[23,24] aromatic,[21] and ionic[22] interactions between organic polymers and inorganic oxides. For instance, the strong hydrogen bond between organic polymers having hydrogen-accepting groups such as poly(2-methyl-2-oxazoline), poly(*N*-vinylpyrrolidone), and poly(*N*,*N*-dimethylacrylamide) and hydrogen-donating moieties of silanol groups from sol−gel reaction resulted in the nanometer scale dispersion of the organic polymer in a silica gel matrix. The obtained hybrid materials were completely amorphous and easily shaped as transparent films and monoliths.

Another new direction involves organizing the organic or inorganic species at the nano/mesoscopic level using supramolecules or self-assembly techniques.[25−37] Nanometric organic, inorganic components, and templates were employed for the preparation of the nanostructured hybrid materials. Our group first reported nanostructured organic−inorganic hybrid materials with starburst dendrimers.[25] A single molecular dendrimer having amide groups was dispersed in a silica gel matrix via strong hydrogen bonds between amide moieties of the dendrimer and silanol groups from tetramethoxysilane (TMOS). Interestingly, the porous silica obtained by calcination of the dendrimer/silica hybrids reflected the generation of the dendrimer. Single π-conjugated polymer filling of silicate mesoporous channels[26−30] gave interesting inorganic replicas via sol−gel nanocoating of templated organogelators,[31,32] π-conjugated disklike molecules,[33] and liquid crystals.[34,35]

Scheme 1

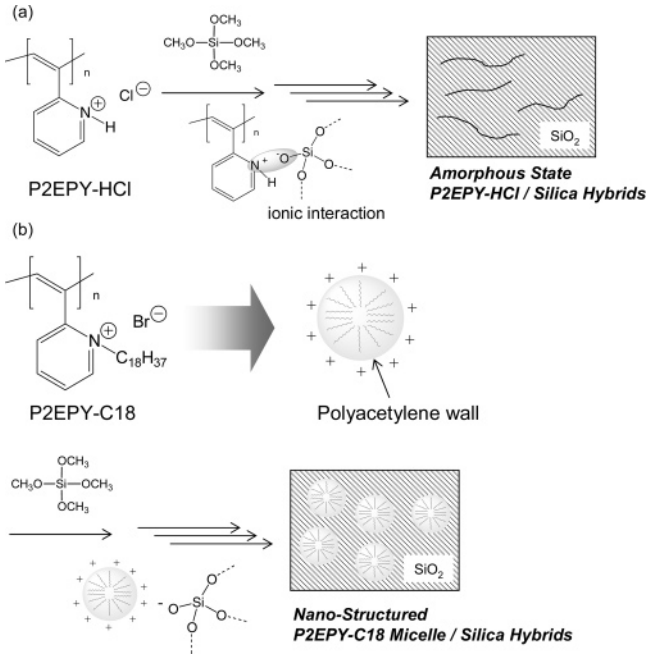

* Corresponding author: Tel +81-75-383-2604; Fax 81-75-383-2605; e-mail chujo@chujo.synchem.kyoto-u.ac.jp.

10.1021/ma050296z CCC: $30.25
Published on Web 09/27/2005

Table 1. Synthesis of P2EPY-HCl/Silica Hybrids[a]

run	P2EPY-HCl (mg)	P2EPY (mg)	TMOS (mg)	MeOH (mL)	appearance	ceramic yield (wt %) calcd	ceramic yield (wt %) obsd[b]
1	25		2000	5	transparent	97.0	89.5
2	25		1000	5	transparent	94.1	82.1
3	25		250	5	transparent	80.0	69.3
4	50		125	5	transparent	50.0	46.6
5		50	125	5	phase separated		

[a] 0.1 M HCl_{aq} (4 equiv to TMOS) was used as a catalyst for sol−gel reaction of TMOS, stirring time was 1 h and the solvent was evaporated at 60 °C. [b] Determined by TGA.

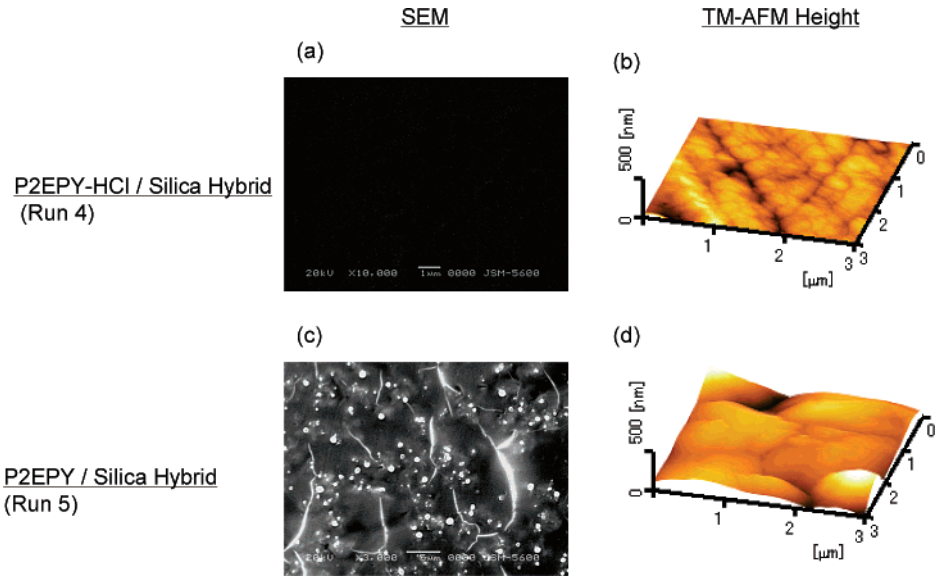

Figure 1. (a, b) The P2EPY−HCl/silica hybrid (run 4) and (c, d) the P2EPY/silica hybrid (run 5), (a, c) SEM images, and (b, d) height images from TM-AFM measurement.

Scheme 2

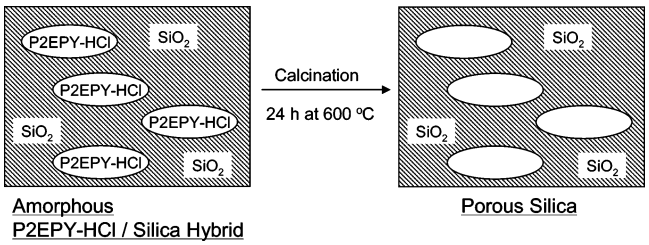

In this article we describe the synthesis of amorphous and nanostructured cationic polyacetylene/silica hybrids by utilizing ionic interactions (Scheme 1). Amorphous poly(2-ethynylpyridinium chloride) (P2EPY-HCl)/silica hybrids were obtained using ionic interactions between the cationic pyridinium groups of P2EPY-HCl and anionic silanol moieties from TMOS (Scheme 1a). In contrast, nanostructured cationic polyacetylene/silica hybrids were synthesized by using self-assembly of poly(*N*-octadecyl-2-ethynylpyridinium bromide) (P2EPY-C18) (Scheme 1b). The conformation of P2EPY-C18 depended greatly on the environment. Under hydrophilic conditions, P2EPY-C18 formed characteristic micelles (about 10 nm). The hydrophobicity of the alkyl chains induced the formation of micelles. Therefore, micelles covered by conducting polyacetylene walls should form in hydrophilic surroundings. To our knowledge, this is the first example of the selective preparation of amorphous and nanometric π-conjugated, conducting polymer/silica hybrids accomplished by self-assembly, while poly(vinylpyridine) polysoap/silica hybrids have been studied already.[36,37] It is expected that the nanometric polyacetylene/silica hybrids will give unique new optical and electronic features compared with amorphous polyacetylene/silica hybrids.

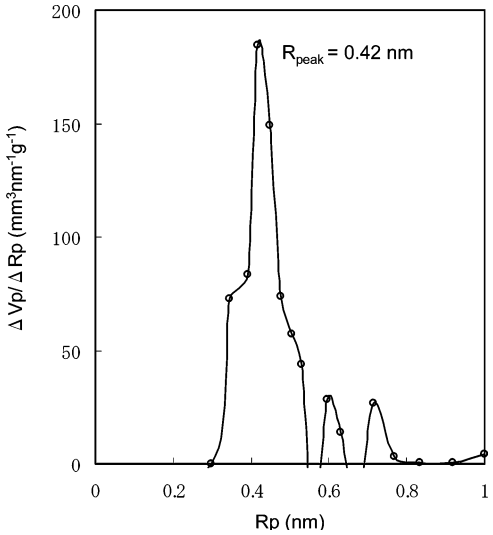

Figure 2. Pore size distribution plot of the porous silica obtained by calcination of the polymer hybrid (run 4).

Experimental Section

Materials. Tetramethoxysilane (TMOS) was distilled and stored under a nitrogen atmosphere. The other solvents and reagents were used as supplied.

Measurements. Thermogravimetric analysis (TGA) was performed using a TG/DTA6200 (SEIKO Instruments, Inc.), with heating rate of 10 °C min^{-1} in air. Scanning electron microscopy (SEM) measurements were conducted using a

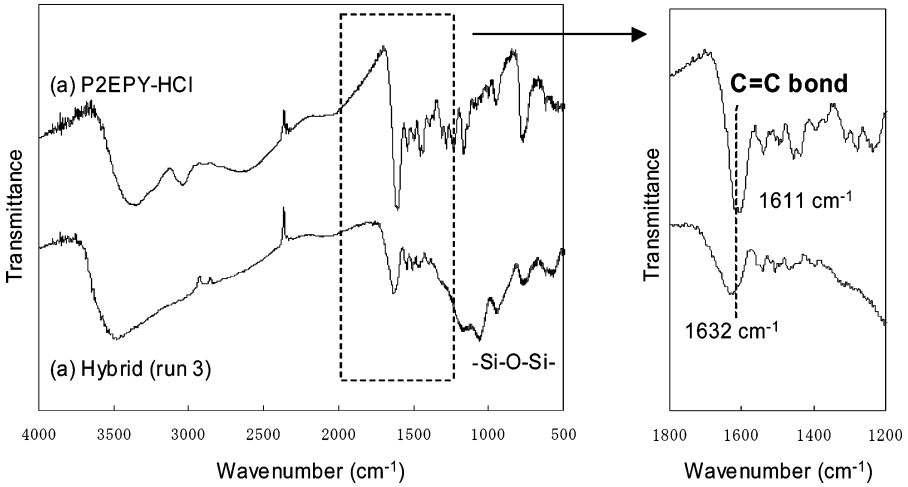

Figure 3. FT-IR spectra of (a) the P2EPY-HCl and (b) the polymer hybrid (run 3).

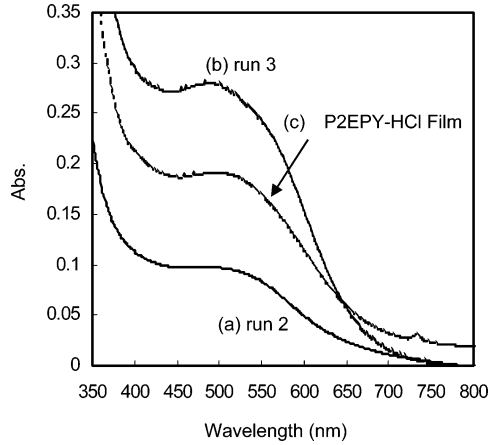

Figure 4. UV spectra of (a) the polymer hybrid (run 2, P2EPY-HCl/silica = 1/16), (b) the polymer hybrid (run 3, P2EPY-HCl/silica = 1/4), and (c) the P2EPY-HCl film.

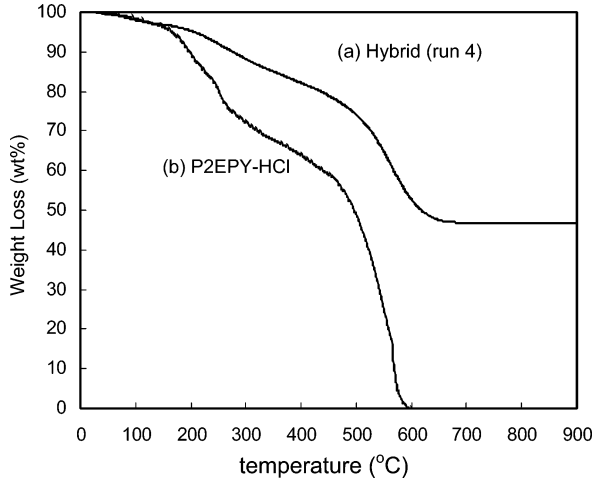

Figure 5. TGA curves of (a) the polymer hybrid (run 4) and (b) the original P2EPY−HCl.

JEOL JNM-5310/LV system. Differential scanning calorimetry (DSC) thermograms were obtained with a DSC200 (SEIKO Instruments, Inc.), with heating rate of 10 °C min^{-1} under a nitrogen atmosphere. The surface images were measured using a tapping mode atomic force microscopy (TM-AFM) (SPA 400, SEIKO Instruments) operating at room temperature. Height and phase images were recorded simultaneously. Nanoprobe cantilevers (SI-DF20, SEIKO Instruments) were utilized. The ^{1}H NMR spectra were recorded on a 400 MHz JEOL EX-400 spectrometer. The FT-IR spectra were obtained using a Perkin-Elmer 1600 infrared spectrometer. Absorption spectra were obtained on a JASCO V-530 spectrometer.

Synthesis of Poly(2-ethynylpyridinium chloride) (P2EPY-HCl), Poly(*N*-octadecyl-2-ethynylpyridinium bromide) (P2EPY-C18), and Poly(2-ethynylpyridine)-(P2EPY). Poly(2-ethynylpyridinium chloride) (P2EPY-HCl), poly(2-ethynylpyridine) (P2EPY), and poly(*N*-octadecyl-2-ethynylpyridinium bromide) (P2EPY-C18) were prepared according to the detailed experimental procedure described in previous literature.[36−41]

Synthesis of Amorphous P2EPY-HCl/Silica Hybrids. A typical preparation procedure of organic−inorganic polymer hybrids with P2EPY-HCl is as follows. P2EPY-HCl and TMOS were dissolved in methanol. To the mixture, aqueous hydrochloric acid (0.1 M) was added. The reaction mixture was stirred for 1 h at room temperature in a sealed bottle. Then, the resulting solution was placed in a container with a paper towel and left in air at 60 °C. A paper towel was used for taking up the solvent and keeping out some dusts from air. After evaporating the solvent completely, the polymer hybrids were obtained as a glassy material. P2EPY-HCl/silica hybrid films for TM-AFM and UV measurements were prepared by casting the reaction mixture on quartz substrate.

Synthesis of Nanostructured P2EPY-C18 Micelles/Silica Hybrids. P2EPY-C18 was dissolved in methanol with the prescribed amount of TMOS and 0.1 M aqueous hydrochloric acid (4 equiv to TMOS). The mixture was stirred for 1 h in a sealed bottle for proceeding of sol−gel reaction. Then, the film of the P2EPY-C18/silica hybrids was prepared on glass slide by the spin-coating method. To proceed sol−gel reaction of TMOS completely, the obtained film was heated at 60 °C for 24 h.

Nitrogen Adsorption Porosimetry. The powder of the polymer hybrid was heated at 600 °C in an ambient atmosphere for 24 h to remove organic components. The sample was dried at 150 °C for 2 h at reduced pressure before porosimetry measurements. The surface area was calculated with the Brunauer−Emmet−Teller (BET)[44] equation in the range of 0.05−0.30 (p/p_0), and the pore size distribution was estimated by the MP method.[45]

Results and Discussion

Amorphous P2EPY-HCl/Silica Hybrids. Table 1 summarizes the results of the preparation of polymer hybrids with P2EPY-HCl. Highly transparent and homogeneous P2EPY-HCl/silica hybrids were obtained over a wide range (runs 1−4). On the other hand, the sample with P2EPY, which was synthesized by the deprotonation of P2EPY-HCl, led to phase separation (run 5). These results indicate strongly that the formation of the ionic interaction between the cationic pyridinium group of P2EPY-HCl and anionic silanol moie-

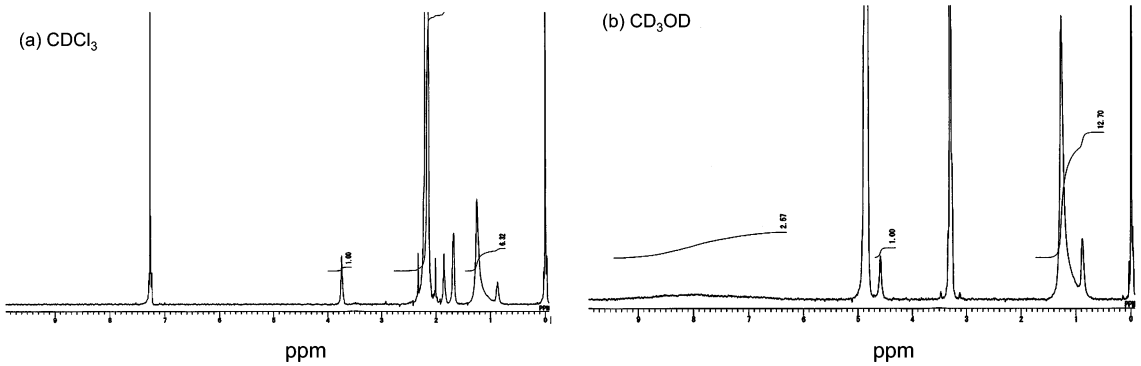

Figure 6. ^1H NMR spectra of P2EPY-C18 in CD_3Cl (a) and in CD_3OD (b).

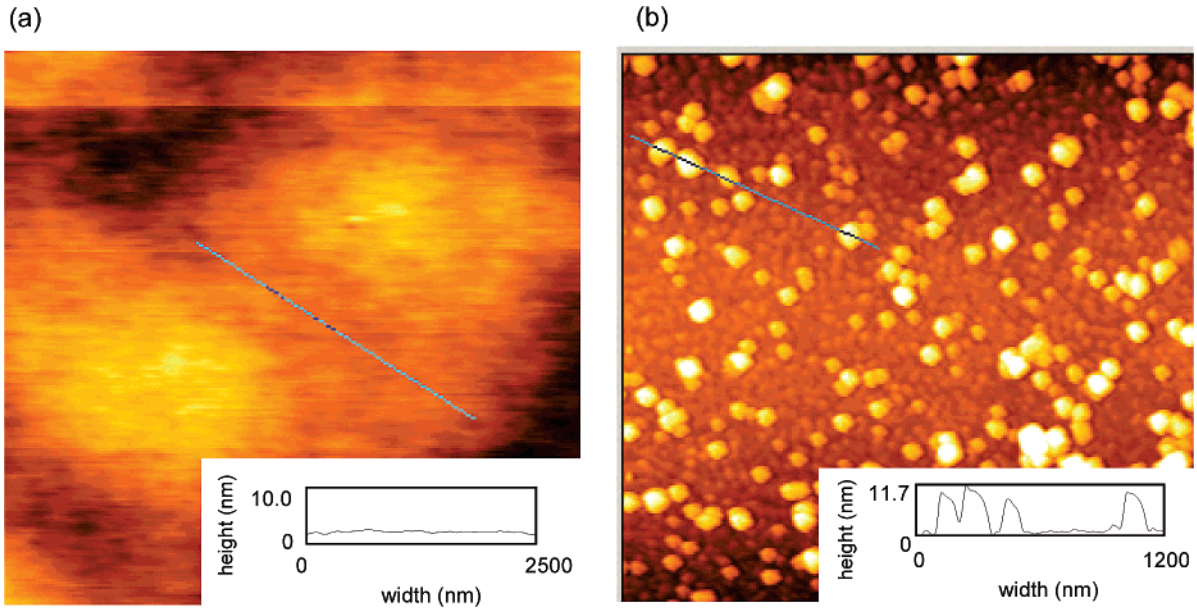

Figure 7. TM-AFM height images of (a) the P2EPY-C18 film from THF (5 μm × 5 μm) and (b) the P2EPY-C18 micelles from methanol (2.5 μm × 2.5 μm). Inset images are the height profiles.

ties of silica is necessary for the preparation of transparent P2EPY-HCl/silica hybrids (Scheme 1a). The ceramic yields were calculated by TGA measurement. The ceramic yields gradually decreased according to decrease in TMOS used. The polymer hybrids were prepared at 60 °C under air in a box condition; therefore, a small amount of TMOS was vaporized before the gelation. Some difference of the calculated value with that of the founded one might be due to this loss of TMOS.

The homogeneity of P2EPY-HCl/silica hybrids was examined by SEM and TM-AFM measurements (Figure 1). The phase-separated P2EPY/silica hybrid (run 5) had aggregations of P2EPY in silica gel matrix (Figure 1c: SEM image) and exhibited high surface roughness (Figure 1d: TM-AFM height image, Rq = 30.1 nm). In contrast, as shown in Figure 1a (SEM image), the polymer hybrid from P2EPY-HCl and TMOS (run 4) showed high homogeneous dispersion of P2EPY-HCl in the silica gel matrix. The surface of the polymer hybrid was very smooth at the nanometer level (Figure 1b: TM-AFM height image, Rq = 3.06 nm). As a previous paper reported, high transparent polymer hybrids showed high homogeneity and very smoothness, which were measured by SEM and TM-AFM. Therefore, these results strongly indicate the high homogeneity of the obtained P2EPY-HCl/silica hybrids

Table 2. Synthesis of Nanostructured P2EPY-C18 Micelle/Silica Hybrids[a]

run	P2EPY-C18 (mg)	TMOS (mg)	MeOH (mL)	THF (mL)
6	20	50	15	
7	20	500	15	
8	20	500		15

[a] 0.1 M HCl_{aq} (4 equiv to TMOS) was used as a catalyst for sol–gel reaction of TMOS, stirring time was 1 h, and the sample was prepared on glass slide by the spin-coating method.

The miscibility between P2EPY-HCl and silica was quantitatively examined by nitrogen adsorption porosimetry study. The porous silica was obtained by burning out organic phase from the polymer hybrid without shrinking of silica gel. Therefore, the size of the porous silica should correspond to the miscibility of organic polymer in the silica gel matrix (Scheme 2). Previous papers have justified the used of this method.[17,20,22,25] The adsorption isotherm curve of porous silica from polymer hybrid (run 4) was classified with a type I curve, suggesting that the porous silica had angstrom pores.[44] The pore size distribution of the porous silica was calculated using the MP method[45] (Figure 2). The porous silica exhibited a strong sharp peak at 0.42 nm, indicating molecular dispersion of P2EPY in the silica gel matrix.

Figure 3 shows the FT-IR spectra of (a) the pristine P2EPY-HCl and (b) the P2EPY-HCl/silica hybrid (run

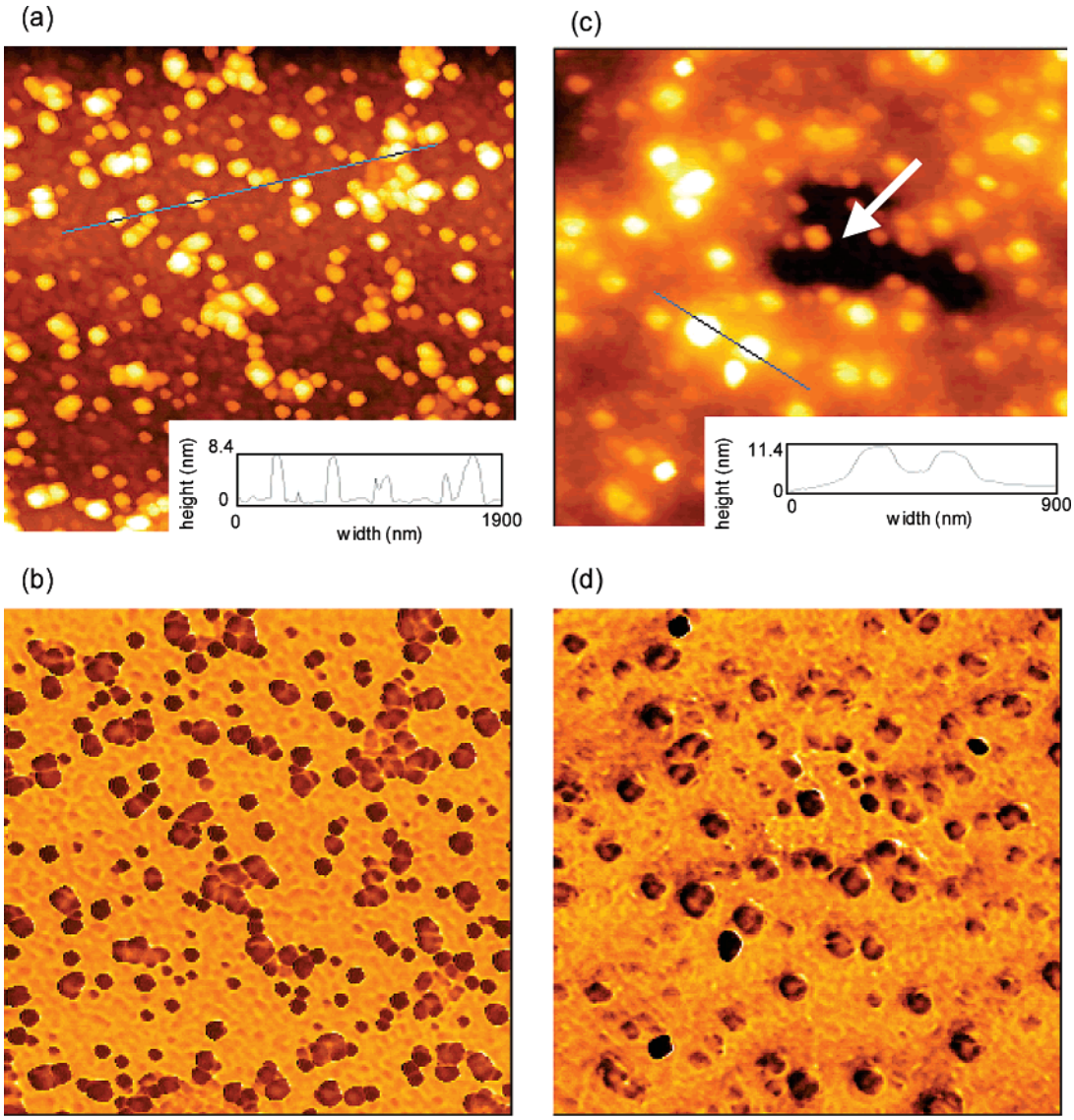

Figure 8. TM-AFM images of (a, b) the P2EPY-C18 micelles/silica hybrid (P2EPY−C18/silica = 1/1, run 6), (c, d) the P2EPY-C18 micelles/silica hybrid (P2EPY-C18/silica = 1/10, run 7), (a, c) height images, (b, d) phase images, 2.5 μm × 2.5 μm. Inset images in (a, c) are height profiles.

3). The stretching band of C=C bond of pristine P2EPY-HCl was observed at 1611 cm^{-1}. In contrast, the stretching band of P2EPY-HCl in silica gel matrix shifts to 1632 cm^{-1}, suggesting a change in the P2EPY-HCl backbone conformation in the silica gel matrix.

To evaluate the optical properties of the amorphous P2EPY-HCl/silica hybrids, UV measurements were carried out (Figure 4). Films of P2EPY-HCl/silica hybrids showed a UV adsorption at 490 nm. The same peak was observed in film of pure P2EPY-HCl (without silica). This indicates that the π-conjugation length of P2EPY-HCl was not affected by the silica gel matrix.

Thermal properties of P2EPY-HCl/silica hybrids were revealed by TGA measurements (Figure 5). The 10 wt % weight loss temperature (T_{10}) of P2EPY-HCl and the P2EPY-HCl/silica hybrid (run 4) was 196 and 276 °C, respectively. The thermal stability of P2EPY-HCl in the polymer hybrid is markedly improved compared with that of bulk P2EPY-HCl.

Nanostructured P2EPY-C18 Micelle/Silica Hybrids. Nanostructured substituted ionic polyacetylene/silica hybrids were prepared using amphiphilic ionic polyacetylene, P2EPY-C18. Since P2EPY-C18 has a hydrophobic octadecyl side chain and hydrophilic pyridinium chloride moieties, P2EPY-C18 should automatically form nanoscopic structures depending on type of solvents. The formation of nanometric organization of P2PEY-C18 was checked by ^{1}H NMR spectra. Figure 6 shows the ^{1}H NMR spectra of P2PEY-C18 in (a) $CDCl_3$ and (b) CD_3OD. While the full octadecyl chain peaks (0.8−1.3, 1.7, 1.8, and 2.0−2.4 ppm) were clearly observed in CD_3Cl, these peaks partially disappeared in CD_3OD. In contrast, the broad peaks (6.5−9.5 ppm) from the pyridinium cation moiety of P2PEY-C18 in CD_3OD could not be found in $CDCl_3$. These ^{1}H NMR observations clearly suggest the formation of nanometer scale organization of P2PEY-C18: In hydrophilic solvent of methanol, the molecular motion of the octadecyl side chain is limited by hydrophilic cationic pyridinium moieties. The nanostructures of P2EPY-C18 depending on the solvent used were revealed by TM-AFM measurement (Figure 7). The samples were prepared on glass slides by using a spin-coating. P2EPY-C18 coating made using THF exhibited no characteristic structure on the nanometer level (Figure 7a). On the other hand, the nanoparticles were clearly observed in the sample

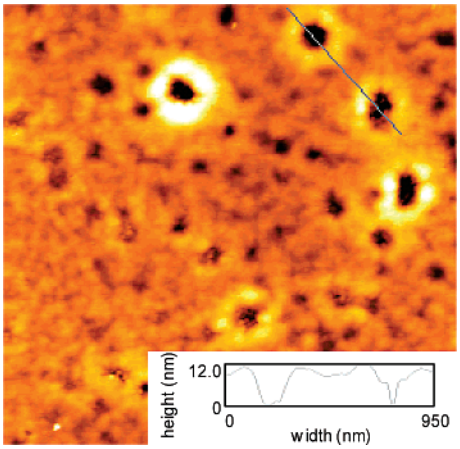

Figure 9. TM-AFM images of the P2EPY−C18 micelles/silica hybrids (P2EPY-C18/silica = 1/10, run 6) after calcination, 2.5 μm × 2.5 μm. Inset image is the height profile.

using methanol (Figure 7b). The height of the particles was about 10 nm from its cross-section image (Figure 7b, inset). Micelles from P2EPY-C18 were visualized as spherical shapes by TM-AFM height images. P2EPY-C18 forms nanometer scale micelle structure in methanol where in the octadecyl side chain segments act as a hydrophobic core and pyridinium cation and doped conducting polyacetylene backbone segments act as a surrounding hydrophilic outer shell. A micelle covered by a conducting polyacetylene wall should form in methanol.

Polyacetylene wall micelle/silica hybrids were prepared (Table 2). The obtained polymer hybrids with P2EPY-C18 in methanol were extremely homogeneous and transparent over wide ranges (runs 6 and 7). In the transparent polymer hybrid (run 7), the characteristic mesostructured image could not be captured via SEM image at 10 000 magnifications. But the nanostructure of the obtained polymer hybrids was clearly visualized by TM-AFM. In the polymer hybrid with a low silica ratio (run 6), micelles at the nanometer level were clearly seen in the TM-AFM height image (Figure 8a). These nanoparticles were also observed in the polymer hybrid with high silica ratio (run 7, Figure 8c), which seemed to be strongly incorporated into a silica gel matrix compared with the hybrid with a low silica ratio (run 6). The part shown by a white arrow was the surface of the substrate. The amorphous state of silica gel matrix including P2EPY-C18 micelles should be found on the surface. The height of P2EPY-C18 micelles on the silica gel matrix was found to be 8−12 nm from the cross-section image (Figure 9a,c, inset images). In addition, phase images (Figure 8b,d) also observed P2EPY-C18 nanoparticles due to the difference of Young's modulus between P2EPY-C18 micelle and silica.

Furthermore, the P2EPY-C18 micelle/silica hybrid (run 7) was heated at 600 °C. By burning out the polymer hybrid at the temperature, the porous silica reflecting the size of P2EPY-C18 micelles was obtained. The surface of the obtained porous silica was measured by TM-AFM. Some pores were found on the surface (Figure 9). The depth of these pores was about 12 nm from the cross-section image (Figure 9, inset image). From these observations, it was confirmed that the nanoparticles found on the surface by TM-AFM measurement were P2EPY-C18 micelles.

Conclusions

Transparent amorphous and nanostructured polymer hybrids with ionic polyacetylene were obtained. The strong ionic interaction between cationic pyridinium groups at the side chain and anionic silanol moieties generated in the sol−gel reaction resulted in the nanometer scale dispersion of the ionic polyacetylene and its micelle in silica gel matrix. The conducting and optical properties depending on the nanostructure of ionic polyacetylene in the silica gel matrix are now under investigation.

References and Notes

(1) Special issues for nanocomposites materials. *Chem. Mater.* **1996**, *8* (8); *Chem. Mater.* **1997**, *9* (11); *Chem. Mater.* **2001**, *13* (10); *MRS Bull.* **2001**, *26* (5).
(2) Schmid, G.; Maihack, V.; Lantermann, F.; Peschel, S. *J. Chem. Soc., Dalton Trans.* **1996**, 589.
(3) Beecroft, L. L.; Ober, C. K. *Chem. Mater.* **1998**, *10*, 1440.
(4) Sanchez, C.; Lebeau, B.; Chaput, F.; Boilot, J.-P. *Adv. Mater.* **2003**, *23*, 1969.
(5) Wen, J.; Wilkes, G. L. *Chem. Mater.* **1996**, *8*, 1667.
(6) Loym, D. A.; Shea, K. J. *Chem. Rev.* **1995**, *95*, 1431.
(7) Novak, B. M. *Adv. Mater.* **1993**, *5*, 422.
(8) Giannelis, E. P. *Adv. Mater.***1996**, *8*, 29.
(9) Corriu, R. J. P. *Angew. Chem., Int. Ed.* **2000**, *39*, 1376.
(10) Boury, B.; Corriu, R. J. P. *Chem. Commun.* **2002**, 795.
(11) Chujo, Y.; Tamaki, R. *MRS Bull.* **2001**, *26*, 389.
(12) Ichinose, I.; Kunitake, T. *Chem. Rec.* **2002**, *2*, 339.
(13) Sanchez, C.; Ribot, F.; Lebeau, B. *J. Mater. Chem.* **1999**, *9*, 35.
(14) Moreau, J. J. E.; Man, M. W. C. *Coord. Chem. Rev.* **1998**, *178−180*, 1073.
(15) Lebeau, B. J.; Sanchez, C. *Curr. Opin. Solid State Mater. Sci.* **1999**, *4*, 1.
(16) Ogoshi, T.; Chujo, Y. *Macromolecules* **2004**, *37*, 5916.
(17) Ogoshi, T.; Chujo, Y. *Macromolecules* **2003**, *36*, 654.
(18) Ogoshi, T.; Itoh, H.; Kim, K. M.; Chujo, Y. *Macromolecules* **2002**, *35*, 334.
(19) Ogoshi, T.; Fujiwara, T.; Bertolucci, M.; Galli, G.; Chiellini, E.; Chujo, Y.; Wynne, K. J. *J. Am. Chem. Soc.* **2004**, *126*, 12284.
(20) Ogoshi, T.; Itoh, H.; Kim, K. M.; Chujo, Y. *Polym. J.* **2003**, *35*, 178.
(21) Tamaki, R.; Samura, K.; Chujo, Y. *Chem. Commun.* **1998**, 1131.
(22) Tamaki, R.; Chujo, Y. *Chem. Mater.* **1993**, *5*, 1113.
(23) Imai, Y.; Itoh, H.; Naka, K.; Chujo, Y. *Macromolecules* **2000**, *33*, 4343.
(24) Imai, Y.; Naka, K.; Chujo, Y. *Polym. J.* **1998**, *30*, 990.
(25) Chujo, Y.; Matsuki, H.; Kure, S.; Saegusa, T.; Yazawa, T. *J. Chem. Soc., Chem. Commun.* **1994**, 635.
(26) Aida, T.; Tajima, K. *Angew. Chem., Int. Ed.* **2001**, *40*, 3803.
(27) Lu, Y.; Yang, Y.; Sellinger, M.; Lu, M.; Huang, J.; Fan, H.; Haddad, R.; Lopez, G.; Burns, A. R.; Sasaki, D. Y.; Shelnutt, J.; Brinker, C. J. *Nature (London)* **2001**, *410*, 913.
(28) Cardin, D. J.; Constantine, S. P.; Gilbert, A.; Lay, A. K.; Alvaro, M.; Galletero, M. S.; Garcia, H.; Marquez, F. *J. Am. Chem. Soc.* **2001**, *123*, 3141.
(29) Lin, V. S. Y.; Radu, D. R.; Han, M. K.; Deng, W.; Kuroki, S.; Shanks, B. H.; Pruski, M. *J. Am. Chem. Soc.* **2002**, *124*, 9040.
(30) Moriguchi, I.; Koga, Y.; Matsukura, R.; Teraoka, Y.; Kodama, M. *Chem. Commun.* **2002**, 1844.
(31) Jung, J. H.; Ono, Y.; Shinkai, S. *J. Am. Chem. Soc.* **2000**, *122*, 5008.
(32) Jung, J. H.; Ono, Y.; Shinkai, S. *Angew. Chem., Int. Ed.* **2000**, *39*, 1862.
(33) Kimura, M.; Wada, K.; Ohta, K.; Hanabusa, K.; Shirai, H.; Kobayashi, N. *J. Am. Chem. Soc.* **2001**, *123*, 2438.
(34) Corriu, R. J. P. *Angew. Chem., Int. Ed.* **2000**, *39*, 1376.
(35) Muramatsu, H.; Corriu, R. J. P.; Boury, B. *J. Am. Chem. Soc.* **2003**, *125*, 854.
(36) Krämer, E.; Förster, S.; Göltner, C.; Antonietti, M. *Langmuir* **1998**, *14*, 2027.
(37) Polarz, S.; Antonietti, M. *Chem. Commun.* **2002**, 2593.
(38) Subramanyam, S.; Blumstein, A.; Li, K.-P. *Macromolecules* **1992**, *25*, 2065.

(39) Zhou, P.; Blumstein, A. *Polymer* **1996**, *37*, 1477.
(40) Okawa, H.; Kurosawa, K.; Wada, T.; Sasabe, H. *Synth. Met.* **1995**, *71*, 1657.
(41) Kim, D. W.; Blumstein, A.; Kumar, J.; Samuelson, L. A.; Kang, B.; Sung, C. *Chem. Mater.* **2002**, *14*, 3925.
(42) Zhou, P.; Samuelson, L.; Alva, K. S.; Chen, C.-C.; Blumstein, R. B.; Blumstein, A. *Macromolecules* **1997**, *30*, 1577.
(43) Sahoo, S. K.; Kim, D. W.; Kumar, J.; Blumstein, A.; Cholli, A. L. *Macromolecules* **2003**, *36*, 2777.
(44) Brunauer, S.; Emmett, P. H.; Teller, E. *J. Am. Chem. Soc.* **1938**, *60*, 309.
(45) Mikhail, R. S.; Brunauer, S.; Bodor, E. E. *J. Colloid Interface Sci.* **1968**, *269*, 45.

MA050296Z